


RESEARCH

Open Access



Disruption of gut integrity and permeability contributes to enteritis in a fish-parasite model: a story told from serum metabolomics

Ariadna Sitjà-Bobadilla^{1,2*} , Rubén Gil-Solsona³, Itziar Estensoro^{1†}, M. Carla Piazzon^{1†}, Juan Antonio Martos-Sitcha^{4,5}, Amparo Picard-Sánchez¹, Juan Fuentes⁶, Juan Vicente Sancho³, Josep A. Calduch-Giner^{2,4}, Félix Hernández^{2,3} and Jaume Pérez-Sánchez^{2,4}

Abstract

Background: In the animal production sector, enteritis is responsible for serious economic losses, and intestinal parasitism is a major stress factor leading to malnutrition and lowered performance and animal production efficiency. The effect of enteric parasites on the gut function of teleost fish, which represent the most ancient bony vertebrates, is far from being understood. The intestinal myxozoan parasite *Enteromyxum leei* dwells between gut epithelial cells and causes severe enteritis in gilthead sea bream (*Sparus aurata*), anorexia, cachexia, growth impairment, reduced marketability and increased mortality.

Methods: This study aimed to outline the gut failure in this fish-parasite model using a multifaceted approach and to find and validate non-lethal serum markers of gut barrier dysfunction. Intestinal integrity was studied in parasitized and non-parasitized fish by immunohistochemistry with specific markers for cellular adhesion (E-cadherin) and tight junctions (Tjp1 and Cldn3) and by functional studies of permeability (oral administration of FITC-dextran) and electrophysiology (Ussing chambers). Serum samples from parasitized and non-parasitized fish were analyzed using non-targeted metabolomics and some significantly altered metabolites were selected to be validated using commercial kits.

Results: The immunodetection of Tjp1 and Cldn3 was significantly lower in the intestine of parasitized fish, while no strong differences were found in E-cadherin. Parasitized fish showed a significant increase in paracellular uptake measured by FITC-dextran detection in serum. Electrophysiology showed a decrease in transepithelial resistance in infected animals, which showed a diarrheic profile. Serum metabolomics revealed 3702 ions, from which the differential expression of 20 identified compounds significantly separated control from infected groups in multivariate analyses. Of these compounds, serum inosine (decreased) and creatine (increased) were identified as relevant and validated with commercial kits.

Conclusions: The results demonstrate the disruption of tight junctions and the loss of gut barrier function, a metabolomic profile of absorption dysfunction and anorexia, which further outline the pathophysiological effects of *E. leei*.

Keywords: Myxozoa, *Enteromyxum leei*, Gilthead sea bream, Teleostei, Aquaculture, Pathophysiology, Tight junctions, Gut barrier, Electrophysiology, Metabolomics

*Correspondence: ariadna.sitja@csic.es

[†]Itziar Estensoro and M. Carla Piazzon contributed equally to this work

¹ Fish Pathology Group, Instituto de Acuicultura Torre de la Sal (IATS-CSIC), 12595 Ribera de Cabanes, Castellón, Spain

Full list of author information is available at the end of the article



Background

Enteritis is the inflammation of the intestine in its broader sense. In humans it can be due to viral, bacterial or parasitic infections, induced by exogenous agents (radiation, medication, drug abuse, etc.), or due to inflammatory conditions such as Crohn's disease or ulcerative colitis. Recent findings also implicate enteric parasites such as *Cryptosporidium parvum* and *Giardia duodenalis* in the development of post-infectious complications such as irritable bowel syndrome and their impact on the neural control of gut functions [1]. In animal production, enteritis is responsible for serious economic losses, intestinal parasitism being a major stress factor leading to malnutrition and lowered performance and production efficiency of livestock and poultry [2]. Furthermore, intestinal health is critically important for welfare and performance in animal production and enteric diseases that cause gut barrier failure result in high economic losses. Common factors in most enteritis scenarios are not only the action of inflammation players, but also the loss of the gut integrity. Intestinal mucus and intercellular tight junctions (TJs) of the epithelial layer act together to maintain the integrity of the gut barrier [3]. The maintenance of the intestinal epithelial barrier is the essential function of the intestinal epithelial cells (IECs), and intraepithelial lymphocytes (IELs) also have sentinel functions in the maintenance of the mucosal barrier integrity [4]. An imbalance in the intestinal barrier structure can flare up into an uncontrollable immune reaction in the intestinal microenvironment or allow the unrestrained growth of microbiota, which leads to various diseases. This loss increases the translocation of bacterial antigens and stimulates inflammation in the intestine [5, 6].

Fish intestine plays various physiological functions that go beyond digestion of food and nutrient absorption. It is also an important immunological site with a key role in protecting the animal from pathogenic insults. Therefore, its integrity is essential to guarantee fish growth, health and welfare [7]. Fish gut integrity has been studied mainly in relation to different dietary interventions that may cause enteritis or several degrees of gut malfunctioning [8–13] and almost no data are available for pathogen-induced enteritis [14]. However, fish intestinal parasitic infections not only cause direct mortalities, but also morbidity, poor growth, higher susceptibility to opportunistic pathogens and lower resistance to stress [15]. The intestinal myxozoan parasite *Enteromyxum leei* dwells between gut epithelial cells and causes severe desquamative enteritis in gilthead sea bream (*Sparus aurata*) (Teleostei), producing anorexia, cachexia, growth impairment, reduced marketability and increased mortality

[16]. In advanced *E. leei* infections, the intestine displays hypertrophy of the lamina propria-submucosa and loss of the epithelial palisade structure, together with an intense local inflammatory response [16–19].

Several techniques have been proposed for studying the morphology and physiology of fish gut [20]. However, most of these techniques are time consuming, or expensive and require lethal samplings. In non-piscine hosts, non-lethal markers have been identified to measure gut barrier failure for some enteric pathogens, under field conditions [21]. In humans, several biomarkers have been used to measure gut permeability and loss of barrier integrity in intestinal diseases, but there remains a need to explore their use in assessing the effect of nutritional factors on gut barrier function. Future studies should aim to establish normal ranges of available biomarkers and their predictive value for gut health in human cohorts [22]. Metabolomics are emerging as a valuable tool to find biomarkers in many diseases, as the metabolome includes all small molecules that are present in a biological system and thus, metabolites serve as direct signatures of the metabolic responses and perturbations in metabolic pathways and tightly correlate with a particular phenotype. These properties make the serum metabolome an attractive minimally invasive technique for the identification of system phenotypic perturbations, especially those disruptions due to pathogens [23, 24], and it has started to be used in aquaculture to identify biomarkers indicative of physiological responses of living organisms to environmental or culture conditions [25–27].

The aim of the present study was to outline the gut failure resulting from a well-characterized enteric fish-parasite model using a multifaceted approach (immunocytochemistry, electrophysiology, gut permeability and metabolomics tools) and to find and validate serum non-lethal markers of gut barrier dysfunction. Thus, serum samples from parasitized and non-parasitized fish were first analysed using non-targeted metabolomics and some significantly altered metabolites were selected to be validated using commercial kits with further samples.

Methods

Fish infection trials and samplings

Juvenile specimens of gilthead sea bream (GSB) (*Sparus aurata*) were obtained from commercial fish farms and transported to IATS-CSIC facilities (Castellón, Spain). Before each trial, 20 fish from each stock were sacrificed and checked by qPCR (*18S* ribosomal RNA gene) [28] and histology to be specific pathogen free and clinically healthy. Animals were acclimatized at least 6 weeks before any intervention and were always kept in 5- μ m-filtered sea water (37.5‰ salinity), with open

flow and natural photoperiod at IATS location (40°5'N, 0°10'E). Temperature was kept constant at 18–19 °C throughout the duration of the trials. Unless stated otherwise, fish were fed *ad libitum* with a commercial diet (EFICO; BioMar, Aarhus, Denmark) throughout all the experiments. Three different trials were performed during this study and are described below. As the parasite dose is not reproducible from one trial to another in this particular model, visual monitoring of clinical signs and non-lethal samplings were performed to evaluate the progression of each infection and select the appropriate timing for a consistent sampling in all trials. The trials are schematically summarized in Fig. 1.

Trial 1 (permeability trial)

GSB with an initial weight of 200 g were exposed to *E. leei*-infected effluent as previously described [29] (recipient group, R; $n=20$) or kept in parasite-free water (control group, C; $n=20$). They were pit-tagged for individual identification and non-lethally sampled at 68 days post-exposure (dpe) for parasite diagnosis (100% prevalence of infection was detected in the R group). At 110 dpe, C ($n=8$; mean weight = 410 g) and R ($n=8$; mean weight = 250 g, with similar infection level at 110 dpe) fish were starved for one day and slightly anesthetized with clove oil (0.1 ml/l) prior to oral intubation with fluorescein isothiocyanate (FITC)-dextran (molecular weight 70 kDa; Sigma-Aldrich, St. Louis, MO, USA) in PBS (dosage = 13 mg/kg of body weight). The two experimental groups were held in separate tanks for 5 h to allow intestinal absorption of the permeability marker. Fish were then sacrificed by overexposure to MS-222 (100 mg/ml; Sigma-Aldrich). Blood was taken from the caudal vessels by puncture with heparinized sterile needles and intestinal segments were collected for histological parasite diagnosis. Blood was allowed to clot for 2 h, then immediately centrifuged (15 min, 3000 × g , 4 °C); the serum was then aliquoted and kept at – 80 °C until analysis.

Trial 2 (electrophysiology trial)

One R group of GSB was anally intubated with 0.4 ml of *E. leei*-infected intestinal scrapings, as previously described [30]. Another C group was intubated with PBS (initial fish weight = 97.5 g). Both groups were non-lethally sampled at 76 days post-intubation (dpi) for parasite diagnosis (95% prevalence of infection was detected in the R group). A final sampling was performed at 107 dpi, where 6 heavily infected R fish (average weight = 114.41 g) and 4 C fish (average weight = 222.8 g) were selected by light microscopy observation of intestinal samples obtained by anal cannulation. Serum and histological samples were taken as described before and a portion of anterior intestine was used for the electrophysiology assay.

Trial 3 (metabolomics trial)

One R group of GSB ($n=25$, initial average weight = 213.04 g) was anally intubated with 1 ml of *E. leei*-infected intestinal scrapings, as in trial 2. Prevalence of infection at the non-lethal (NL) sampling (28 dpi) was 100%. A final lethal sampling was done at 77 dpi, in which serum and intestinal samples were taken for metabolomics and histological diagnosis, respectively, from R ($n=24$, 215.91 g) and C ($n=24$, 312.54 g) fish.

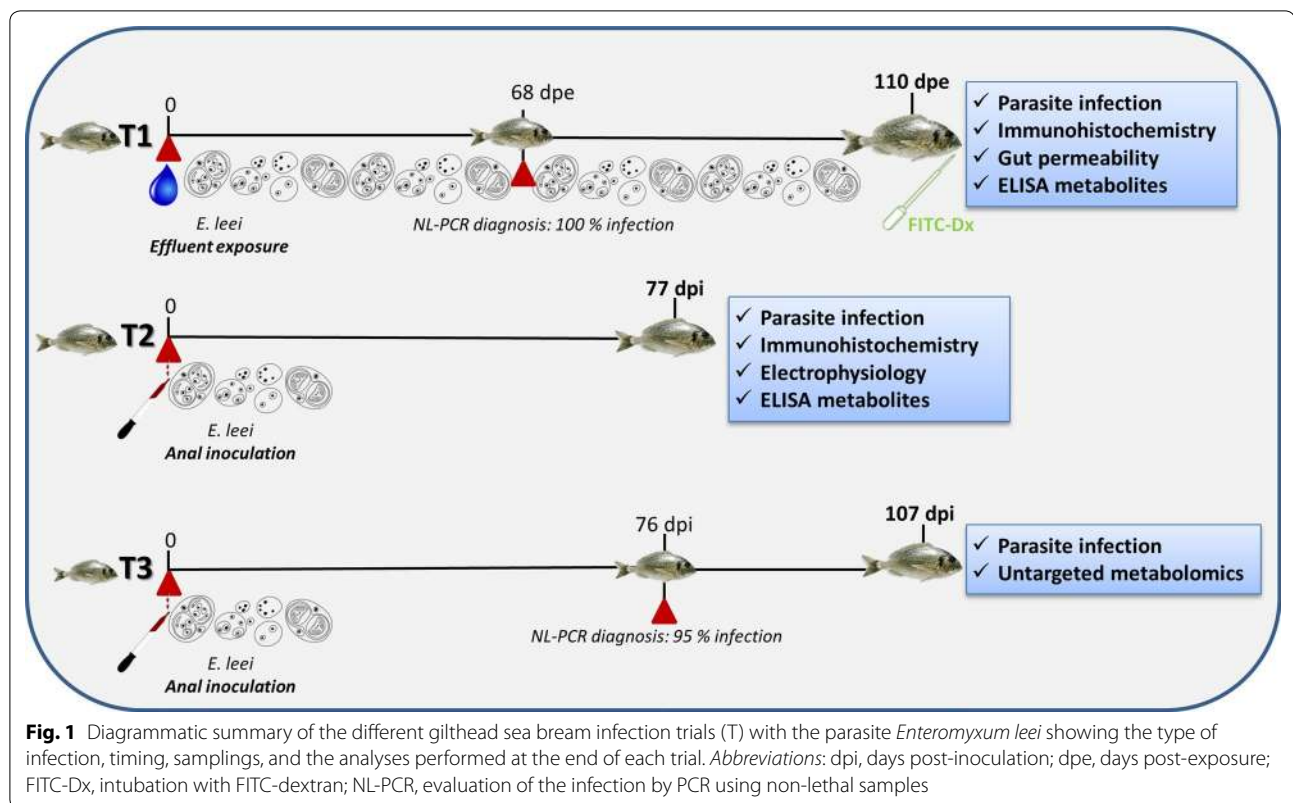
Parasite diagnosis

In all trials, parasite diagnosis was performed on anterior (AI) and posterior (PI) intestinal segments fixed in 10% buffered formalin, embedded in paraffin, 4 μ m-sectioned and stained with Giemsa following standard procedures. Infection intensity was semiquantitatively evaluated in each intestinal segment using a scale from 1 (lowest) to 6 (highest) as previously described [30]. Non-infected segments were scored as 0. All infected fish had high scores in the posterior intestine, the first segment colonized by this parasite. Based on anterior intestine scores, scores of 1–2, 3–4 and 5–6 were considered low, medium and high infection intensities, respectively. All fish from trials 1 and 2 showed high levels of infection. In trial 3, fish showed different degrees of infection and were grouped accordingly for further analysis.

Immunohistochemistry (IHC)

In order to evaluate the intestinal damage induced by the parasite, immunohistochemistry was performed using three different markers involved in epithelial integrity: E-cadherin (CDH1), tight junction protein 1 (TJP1 or ZO-1) and claudin-3 (CLDN3). Commercial cross-reacting antibodies were selected for the three molecules, by comparing the sequence of their epitopes with the sequence available in the gilthead sea bream genomic and transcriptomic databases (<http://www.nutrigroup-iats.org/seabreamdb/>). The selection threshold for the heterologous antibodies was set at 80% of sequence similarity, with long stretches of identical amino acids. In addition, cross-reactivity with undesired proteins was ruled out by blasting the databases.

Four-micrometer-thick sections of anterior, middle and posterior intestine sections from trials 1 and 2 were collected on Super-Frost-plus microscope slides (Menzel-Gläser, Braunschweig, Germany), dried overnight, deparaffinized and hydrated. From each experiment, 4 C and 4 R fish were analyzed. All incubations were performed in a humid chamber at room temperature and washing steps consisted of 5 min immersion in TTBS [20 mM Tris-HCl, 0.5 M NaCl, pH 7.4 (TBS) and 0.05% Tween 20] and 5 min immersion in TBS. Endogenous peroxidase activity was blocked by incubation in



hydrogen peroxide 0.3% v/v in methanol (H_2O_2 :methanol in a 1:9 proportion) for 30 min. Antigen retrieval was performed by boiling the samples in Target Retrieval Solution, pH9 (DAKO, Santa Clara, CA, USA) using a pressure boiler for 30 min. Slides were then washed and blocked 30 min with TBS 1.5% normal goat serum (Vector Laboratories, Burlingame, CA, USA) for the antibodies raised in rabbit (anti-TJP1 and anti-CLDN3) or with TBS 5% BSA for the antibody raised in mouse (anti-CDH1). After washing, slides were incubated with the primary antibodies diluted in TBS 1% BSA for 2 h. The dilutions used were 1:200 for the polyclonal rabbit anti-TJP1 (HPA001636; Sigma-Aldrich) and 1:100 for the polyclonal rabbit anti-CLDN3 (MBS126688; MyBioSource, San Diego, CA, USA). The monoclonal mouse anti-E-cadherin (DAKO, clone NCH-38) was used undiluted and following the protocol previously described [31]. Samples were washed again and incubated with a goat anti-rabbit or a horse anti-mouse antibody (Vector Laboratories) 1:200 in TBS 1.5% normal goat or horse serum, respectively, for 1 h. Slides were subsequently washed and incubated for 30 min with the avidin-biotin-peroxidase complex (ABC, Vector Laboratories), washed and developed by incubating with 3,3'-diaminobenzidine tetrahydrochloride chromogen (DAB; Sigma-Aldrich) for 2 min. The reaction was stopped with deionized water

and the slides were counterstained for 2 min with Gill's haematoxylin before being dehydrated and mounted for light microscopy examination.

Gut permeability assay

Duplicates of individual sera from R and C fish from trial 1 were diluted 1:1 in PBS, dispensed (100 μ l) in 96-well microplates (Thermo Fisher Scientific, Waltham, MA, USA) and read against a standard curve using a range of FITC-dextran concentrations from 2.5 ng/ml to 100 ng/ml. Serum FITC-dextran concentrations were calculated after measuring fluorescence intensity at $\lambda_{em}/\lambda_{ex}$ = 535/485 nm in a microplate reader (Tecan Group Ltd., Männedorf, Switzerland).

Electrophysiology assay

The anterior intestine of C ($n=4$) and R ($n=6$) fish from trial 2 was collected, isolated and mounted in Ussing chambers as previously described [32, 33]. Briefly, tissue was washed with chilled saline, opened flat, placed on a tissue holder of 0.71 cm^2 and positioned between two half-chambers containing 2 ml of physiological saline (NaCl 160 mM; $MgSO_4$ 1 mM; NaH_2PO_4 2 mM; $CaCl_2$ 1.5 mM; $NaHCO_3$ 5 mM; KCl 3 mM; glucose 5.5 mM; HEPES (4-(2-hydroxyethyl)piperazine-1-ethanesulfonic acid, N-(2-hydroxyethyl)piperazine-N'-(2-ethanesulfonic

acid) 4 mM), at a pH of 7.8. During the experiments the tissue was bilaterally gassed with 0.3% CO₂ + 99.7 O₂ and the temperature maintained at 17 °C. Short-circuit current (I_{sc}, μA/cm²) was automatically monitored by clamping epithelia to 0 mV and epithelial resistance (R_t, Ω cm²) was manually calculated (Ohm's law) using the current deflections induced by a 2 mV pulse of 3 s every minute. Voltage clamping and current injections were performed by means of VCC600 or VCCMC2 amplifiers (Physiologic Instruments, San Diego, CA, USA). Bioelectrical parameters for each tissue were manually recorded at 30 min intervals for 150 min after mounting, and data is presented as average of values for each individual.

Untargeted serum metabolomics

Blood (3 ml) from C and R fish from trial 3 was directly collected into clot activator tubes (BD Vacutainer; BD, Madrid, Spain) and kept on ice for 2 h. After centrifugation (15 min at 3000 × g, 4 °C), serum samples were aliquoted and stored at -80 °C until use as described elsewhere [26]. Briefly, one aliquot was deproteinized with acetonitrile for hydrophilic interaction liquid chromatography (HILIC). A second aliquot was evaporated to dryness after acetonitrile deproteinization, and redissolved in methanol 10% for reverse phase (RP) chromatographic analysis. Extracts were then injected in both positive and negative ionization modes (0.7 and 1.5 kV capillary voltages, respectively) in a hybrid quadrupole time-of-flight mass spectrometer (Xevo G2 QTOF; Waters, Manchester, UK) with a cone voltage of 25 V, using nitrogen as both desolvation and nebulizing gas. LC-MS data were processed using the XCMS R package (<https://xcmsonline.scripps.edu>) with Centwave algorithm for peak picking (peak width from 5 to 20 s, S/N ratio higher than 10 and mass tolerance of 15 ppm), followed by retention time alignment, peak area normalization (mean centering), log₂ applying (to avoid heteroscedasticity) and Pareto scaling. For elucidation purposes, fragmentation spectra of features of interest were compared with reference spectra databases (METLIN, <http://metlin.scripps.edu>; Human Metabolome DataBase, <http://www.hmdb.ca>; MassBank, <http://www.massbank.eu>). For unassigned metabolites, *in silico* fragmentation software (MetFrag, <http://msbi.ipb-halle.de/MetFrag>), with subsequent searches through Chemspider (<http://www.chemspider.com>) and PubChem (<https://pubchem.ncbi.nlm.nih.gov>) chemical databases, was employed.

Targeted metabolite detection in serum samples

The concentration of creatine and inosine were measured in serum samples of C and R fish from trials 1 and

2 using specific kits. These two metabolites were selected due to the availability of commercial kits to measure their concentration in serum samples and their significant differential abundance and presence among the VIP variables from the untargeted metabolomics study (see below). Creatine was measured with the Creatine Assay Kit (KA1666; Abnova, Heidelberg, Germany) using 10 μl of each serum sample in duplicate following the manufacturer's instructions. A calibration curve ranging from 0.5 to 50 μM of creatine was included in the assay and the concentration in each sample was extrapolated after measuring fluorescence intensity at λ_{em}/ex = 590/530 nm. Inosine was measured using an Inosine Assay Kit (MAK100; Sigma-Aldrich) using 5 μl of each serum sample in duplicate, following the manufacturer's instructions. A calibration curve ranging from 0.1 to 0.5 nmol/well was included in each assay and the presence of inosine was determined measuring the fluorescence intensity at λ_{em}/ex = 590/530 nm.

Statistics and data analyses

Data from the electrophysiology, gut permeability assays and metabolite detection by ELISA were analysed for statistically significant differences between C and R groups by Student's t-test or the Mann-Whitney test when Shapiro-Wilk normality test failed, using SigmaPlot v.13.0 (Systat Software, San Jose, CA, USA). Differences were considered significant at *P* < 0.05. To study the separation among experimental groups, partial least-squares discriminant analysis (PLS-DA) was performed using EZinfo v.3.0 (Umetrics, Umeå, Sweden). The quality of the PLS-DA model was evaluated by the parameters R²Y(cum) and Q²Y(cum), which indicate the fit and prediction ability, respectively. To discard the possibility of over-fitting of the supervised model, a validation test consisting in 999 random permutations was performed using SIMCA-P+ v.11.0 (Umetrics). The contribution of the different metabolites to the group separation was determined by variable importance in projection (VIP) measurements. A VIP score > 1 was considered to be an adequate threshold to determine discriminant variables in the PLS-DA model [34, 35].

Results

Tight junction protein 1 and claudin 3 protein expression is affected by *E. ileyi*

CLDN3 is an integral membrane protein component of TJ proteins, contributing to create an ion-selective border between apical and basolateral compartments. Thus, as expected, the anti-CLDN3 antibody marked strongly the basal membrane of the intestinal

epithelium and the lateral membranes of enterocytes in the three intestinal segments of control fish, although it was stronger at the AI (Fig. 2a, left pictures). By contrast, the immunolabelling decreased in parasitized intestines (in all intestinal segments), particularly at the lateral junctions at the PI (Fig. 2b, left pictures).

TJP1 is an important intracellular TJ protein, linking the cell cytoskeleton to the transmembrane TJ proteins. The anti-TJP1 antibody marked strongly the basal membrane and the apical epithelium, with a dot-lined style, in all intestinal segments of control animals, being higher at the AI (Fig. 2a, middle pictures). In parasitized fish, however, the immunolabelling was not so strong and decreased similarly in all the sites. It is remarkable that some parasitic stages (secondary and tertiary cells) were also strongly labelled with this antibody (Fig. 2a, b, middle pictures).

CDH1 is a transmembrane protein that acts as a cell adhesion molecule, important in the formation of adherens junctions to bind cells with each other. The anti-CDH1 antibody stained similarly the lateral junction of enterocytes in all intestinal segments of control fish, and the labelling hardly changed in parasitized fish (Fig. 2a, b, right pictures).

Parasitized fish showed an increased intestinal permeability

The paracellular transport of small macromolecules across the intestinal epithelium was assessed through the translocation of 70 kDa FITC-dextran into the blood stream. The FITC-dextran concentration in blood serum of R fish was significantly higher than in C fish (Mann-Whitney U-test: $U_{(8)}=6$, $Z=-2.83$, $P=0.0047$) (Fig. 3). All R fish used for this analysis were infected at the three intestinal segments with high infection intensity.

Intestinal transepithelial resistance is lower in parasitized fish

R_t ($\Omega \text{ cm}^2$), a measure of tissue integrity, was monitored for each AI *ex vivo*. In C fish, R_t steadily raised until 90 min after mounting, as expected, and remained stable thereafter. However, in R fish R_t values remained low and stable throughout the testing time (data not shown). The mean R_t values of the stabilized measurements were significantly higher in C than in R fish (Mann-Whitney U-test: $U_{(4)}=24$, $Z=2.59$, $P=0.0095$) (Fig. 4a). In addition, short circuit current (I_{sc} , $\mu\text{A}/\text{cm}^2$) was also recorded for each epithelial preparation (t-test: $t_{(8)}=3.95$, $P=0.0042$) (Fig. 4b). Under the current experimental conditions, positive I_{sc} values are associated with absorptive function as it was detected in C fish, whereas

the negative I_{sc} values found in R fish indicate a secretory function, reflecting the prevailing electrolyte transport across the epithelium. Thus, C fish exhibited an absorptive (positive) current that reflects a proper function of the epithelium, whereas infection induced a persistent and non-reversed secretory current throughout the measuring period reflecting an *in vivo* persistent diarrhea (negative mean values for R group).

Parasitized fish show significant changes in their serum metabolomics profile

A total of 3702 ions were detected in all four injections (reversed phase and HILIC chromatographies in both positive and negative ionization modes). Among them, 182 showed a P (corrected) higher than 0.5 in a OPLS-DA statistical method, so they were selected for further study (Additional file 1: Figure S1). Some of them showed differences between molecular ion isotopes of 0.5, 0.33 or 0.25 mDa, which were considered peptides or protein fragments with more than a single charge. However, their small intensity made their identification by means of tandem MS really difficult, hampering their final elucidation. Other compounds highlighted by OPLS-DA were studied in MS/MS experiments at 10, 20, 30 and 40 eV collision energy, obtaining a list of 20 tentatively elucidated compounds (Table 1), related to different biological processes [fatty acid oxidation (5 compounds), amino acid catabolism (4 compounds), energy homeostasis (1 compounds), nucleoside metabolism (2 compounds), lysophospholipid metabolism (4 compounds) and vitamins and polyphenols metabolism (4 compounds)]. The differential expression of these 20 identified compounds markedly separated control from infected groups in multivariate analyses (PLS-DA), in which the three first components explained more than 90% and predicted more than 75% of the variance. This analysis separated also R groups by low/medium and high intensity of infection (Fig. 5), although the statistical significance of the prediction was restricted by the number of fish in each R group category.

Inosine and creatine are good serum markers of parasitized fish

The application of the commercial ELISA kits for inosine and creatine showed significant changes in the serum of parasitized fish. The values of fish from trials 1 and 2 were merged to have a higher sample size and statistical robustness (C: $n=8$; R: $n=20$). Inosine was significantly decreased (Mann-Whitney U-test: $U_{(8)}=38$, $Z=2.01$, $P=0.045$) (Fig. 6a), whereas creatine increased (Mann-Whitney U-test: $U_{(7)}=11$, $Z=-3.53$, $P=0.0004$) (Fig. 6b) in parasitized fish.

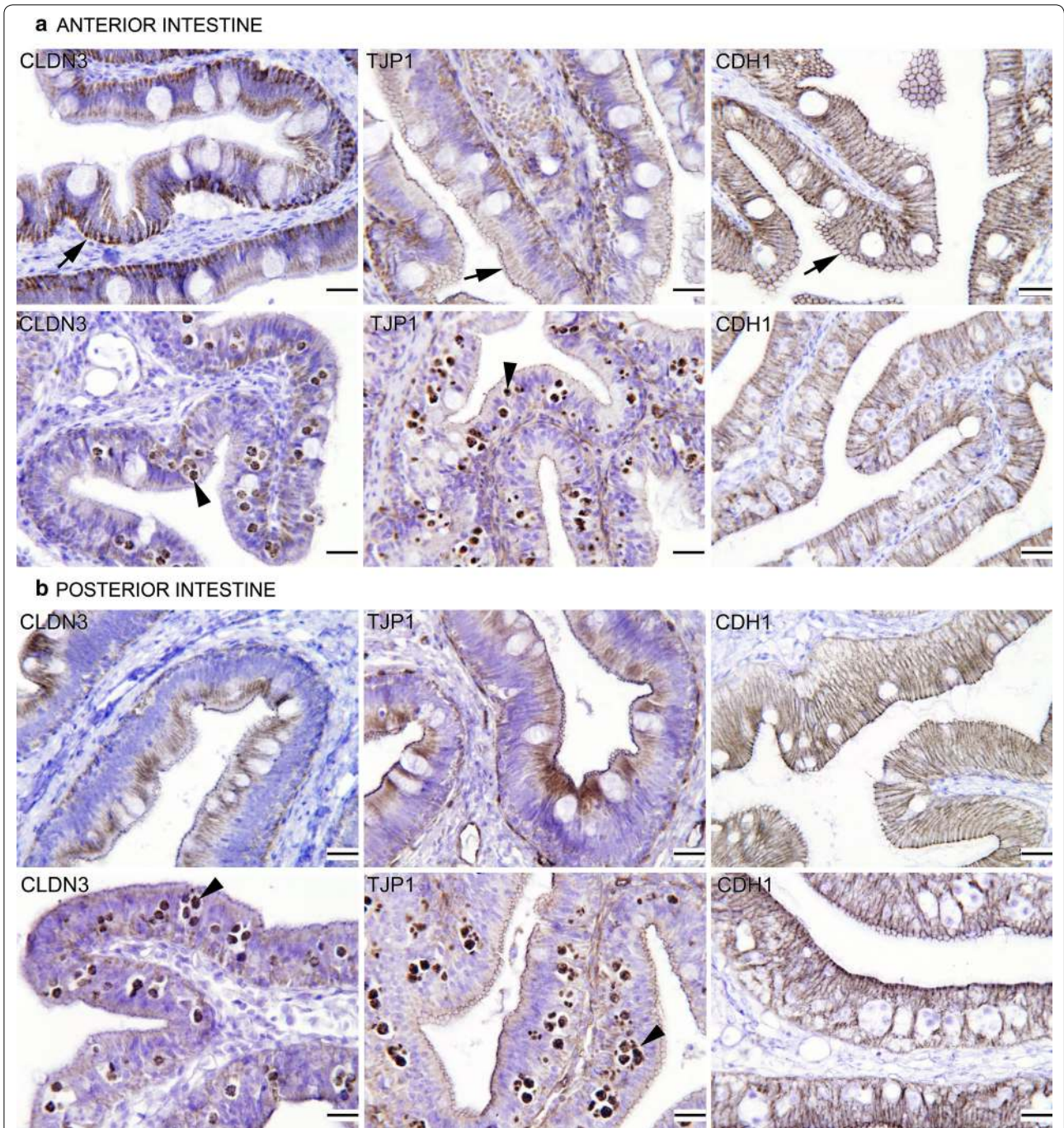
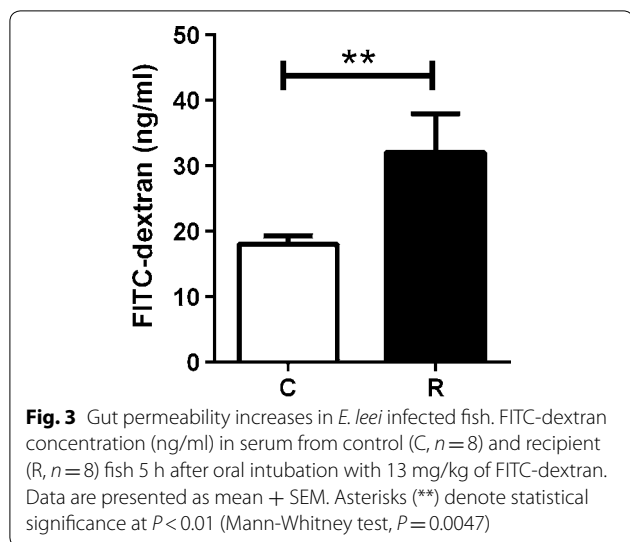


Fig. 2 Photomicrographs of gilthead sea bream sections of anterior (**a**) and posterior (**b**) intestines immunolabelled (brownish colour) with antibodies against claudin 3 (CLDN3, left pictures), tight junction protein 1 (TJP1, central pictures) and E-cadherin (CDH1, right pictures). For each intestinal segment, the upper panel corresponds to control healthy fish and the lower panel to *Enteromyxum leei*-parasitized fish. Arrowheads point to some labelled parasitic stages, and arrows to some of the positive immunostaining of control fish at the anterior intestine. Note the differences in the distribution and staining intensity in parasitized intestinal sections. *Scale-bars*: 20 μ m



Discussion

The gastrointestinal (GI) tract acts as a barrier between the external and internal environments and thus the integrity of this barrier is crucial to maintain homeostasis. The barrier function of the gut is supported by epithelial cells, mucus, tight junction (TJ) and adherens junction (AJ) proteins [36]. The fish-parasite system used in the present study provides an excellent model to study the disruption of this barrier, as *E. leei* dwells in the paracellular space of the gut epithelial palisade. First of all, we have shown the functional disruption of the gut through the increased gut permeability and the decreased

transepithelial resistance in parasitized fish. Secondly, we have demonstrated by IHC the decreased presence of some TJ proteins that are the building blocks of the gut barrier, especially claudin-3. Finally, we have outlined the utility of non-targeted serum metabolomics to detect marker metabolites of the disease condition and we have validated the use of creatine and inosine as disease markers of enteritis.

Epithelial permeability function has been assessed in mammals by *in vitro* or *ex vivo* methods such as transepithelial electrical resistance and *in vivo* tests such as transepithelial passage of different markers [22, 37, 38]. Intestinal mucosal barrier permeability is considered as an effective indicator of the integrity of the mucosal barrier. Experiments on intestinal barrier permeability in fish have been mainly based on *in vitro* and molecular studies such as gene expression studies [11, 13, 39, 40] and very few studies are available using *in vivo* markers [14, 41]. Among the *in vivo* methods, FITC-dextran are primarily used for studying permeability and transport in tissues and cells, but to the best of our knowledge this is the first time that it is used in fish gut studies. Here, we chose a molecular size that allows studying the intestinal paracellular transport, as we hypothesised that the parasite location was altering it (either blocking or favouring). Indeed, what we found was a leaking effect, as the FITC-dextran was increased in the plasma of parasitized fish. Similarly, intestinal permeability was significantly elevated in different fish species after an infectious pancreatic necrosis virus (IPNV) challenge [42] and the paracellular permeability for Evans blue and D-lactate

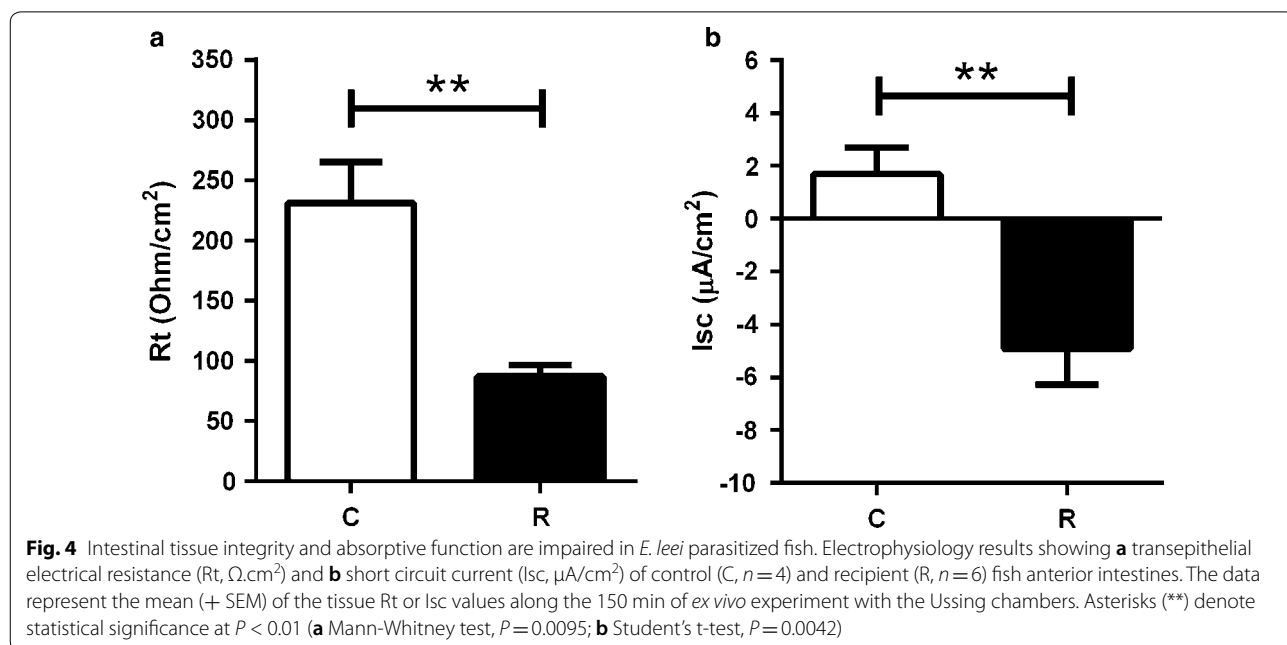


Table 1 Highlighted (↑, upregulated; ↓, downregulated) compounds obtained from untargeted metabolomics of serum samples of gilthead sea bream inoculated with *Enteromyxum leei*. Non-infected (C) fish were compared with highly (R-H) or low/moderately (R-L/M) infected recipient (R) fish

Compound	Biological process [#]	Feature name	Chromatography/ionization mode	Formula	m/z (Da)	R-H, % C	R-L/M, % C	Corrected P-value*
Isobutyryl carnitine ↑	1	M232T96_RPPOS	RP/+	C ₁₁ H ₂₁ NO ₄	232.2967	1615 ^b	969 ^c	6.78E ⁻³
Pivaloylcarnitine ↑	1	M246T150_RPPOS	RP/+	C ₁₂ H ₂₃ NO ₄	245.3153	1128 ^b	664 ^c	5.72E ⁻³
2-methylbutyrylcarnitine ↑	1	M246T155_RPPOS	RP/+	C ₁₂ H ₂₃ NO ₄	246.3233	955 ^b	470 ^c	1.42E ⁻²
Myristoylcarnitine ↑	1	M372T767_RPPOS	RP/+	C ₂₁ H ₄₁ NO ₄	372.5625	303 ^b	127 ^a	3.37E ⁻²
(c18:1)oylcarnitine ↓	1	M426T788_RPPOS	RP/+	C ₂₅ H ₄₇ NO ₄	426.3571	32 ^b	36 ^b	6.21E ⁻⁰³
Oxoadipic acid ↑	2	M159T74_RPNEG	RP/-	C ₆ H ₈ O ₅	159.1168	4704 ^b	8660 ^c	1.63E ⁻²
Leucinic acid ↑	2	M131T254_RPNEG	RP/-	C ₆ H ₁₂ O ₃	131.1497	949 ^b	632 ^c	1.39E ⁻²
γ-Glu-Val ↑	2	M247T94_RPPOS	RP/+	C ₁₀ H ₁₈ N ₂ O ₅	247.2683	402 ^b	202 ^c	7.33E ⁻³
γ-Glu-Ile ↑	2	M261T171_RPPOS	RP/+	C ₁₁ H ₂₀ N ₂ O ₅	259.2790	343 ^b	255 ^b	2.60E ⁻²
Creatine ↑	3	M132T73_RPPOS	RP/+	C ₄ H ₉ N ₃ O ₂	132.1411	425 ^b	245 ^c	1.26E ⁻²
Inosine ↓	4	M267T72_RPNEG	RP/-	C ₁₀ H ₁₂ N ₄ O	203.2205	94 ^a	77 ^b	2.37E ⁻²
Guanosine ↓	4	M282T73_RPNEG	RP/-	C ₁₀ H ₁₃ N ₅ O ₅	282.2328	70 ^a	58 ^b	4.42E ⁻²
LysoPC(20:4) ↓	5	M544T874_RPPOS	RP/+	C ₂₈ H ₅₀ NO ₇ P	543.6729	67 ^b	46 ^b	6.13E ⁻²
LysoPE(18:2) ↑	5	M478T906_RPNEG	RP/-	C ₂₃ H ₄₄ NO ₇ P	476.5638	199 ^b	106 ^a	1.31E ⁻²
LysoPE(16:0) ↑	5	M452T895_RPNEG	RP/-	C ₂₁ H ₄₄ NO ₇ P	454.5583	259 ^b	143 ^b	4.05E ⁻³
LysoPE(18:1) ↑	5	M480T944_RPNEG	RP/-	C ₂₃ H ₄₆ NO ₇ P	480.5855	185 ^b	123 ^a	2.14E ⁻²
Biotin (vitamin B7) ↓	6	M245T223_RPPOS	RP/+	C ₁₀ H ₁₆ N ₂ O ₃ S	245.3186	28 ^b	66 ^c	2.69E ⁻²
Pantothenic acid (vitamin B5) ↓	6	M220T115_RPPOS	RP/+	C ₉ H ₁₇ NO ₅	220.2429	27 ^b	71 ^c	3.56E ⁻²
Delta-valerolactam ↓	6	M100T100_RPPOS	RP/+	C ₅ H ₉ NO	100.1390	16 ^b	38 ^c	6.72E ⁻³
p-aminobenzoic acid (PABA) ↑	6	M138T94_RPPOS	RP/+	C ₇ H ₇ NO ₂	137.0474	177 ^b	215 ^b	1.44E ⁻²

[#] 1, fatty acid oxidation; 2, amino acid catabolism; 3, energy homeostasis; 4, nucleoside metabolism; 5, lysophospholid metabolism; 6, vitamins and polyphenols metabolism

*Benjamini-Hochberg multiple testing correction

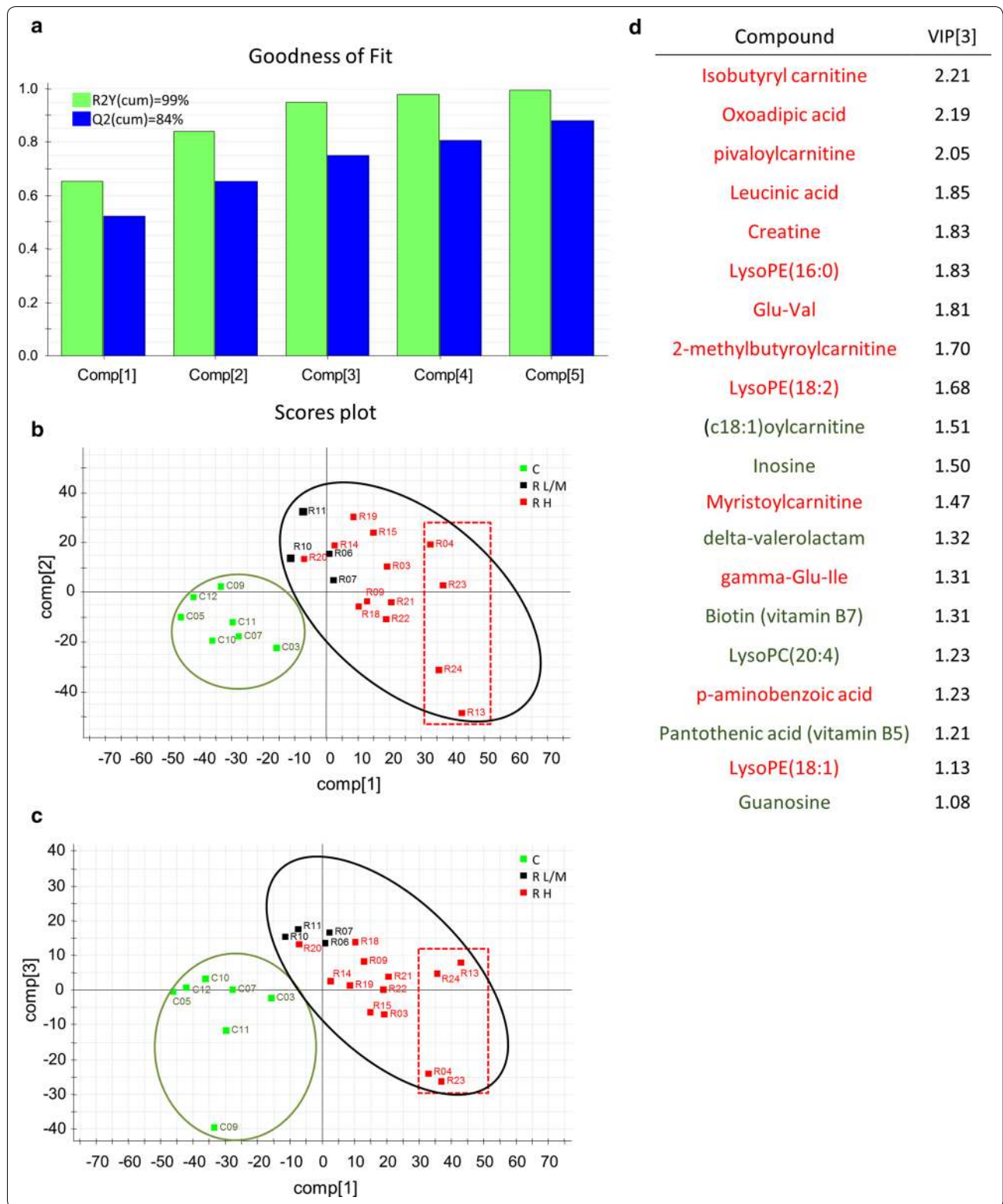
Note: Superscript letters indicate statistically significant differences, using letter ^a for C group

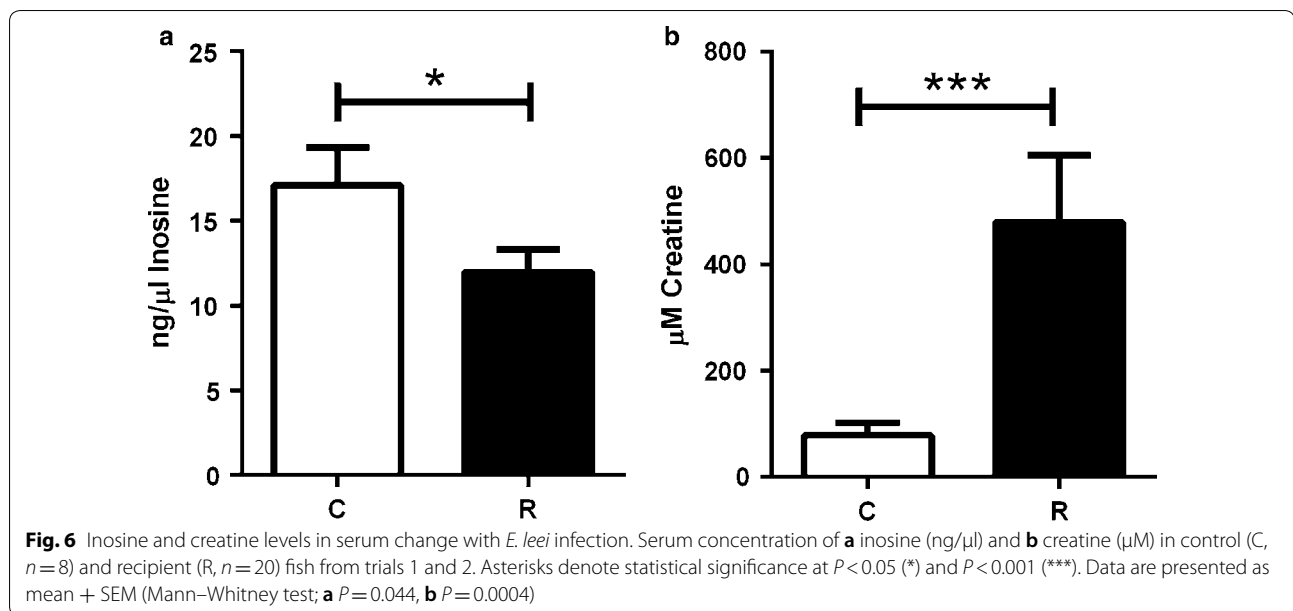
were significantly higher at both 24 and 72 h post-infection with *Aeromonas hydrophila* [14]. The leaking effect was confirmed by the decreased transepithelial resistance in parasitized intestines. These results agree with previous studies showing that *E. leei* disrupts intestinal water uptake, as a significant negative correlation between plasma chloride concentration and condition factor. Thus, a significantly higher osmolarity of plasma and major ion concentrations of the intestinal fluid were found in *E. leei*-infected tiger puffer (*Takifugu rubripes*) [43]. Some fish diets containing high levels of alternative

vegetal protein sources may also induce digestive disturbances including diarrhoea-like conditions, indicating impaired gut permeability of water [44, 45]. Similarly, in GSB, some extreme vegetable diets impair Rt and this negative effect can be overcome when a butyrate additive is added [33]. Several human enteric protozoan parasites typically induce diarrhoea by a combination of different actions that alter gut integrity. For example, *Entamoeba histolytica* degrades the protective mucus layers and evokes mucus hypersecretion. Its interaction with epithelial cells directly induces pro-inflammatory responses

(See figure on next page.)

Fig. 5 PLS-DA analysis of serum metabolomics. **a** Graphical representation of the goodness-of-fit. The three first components explained more than 90% and predicted more than 75% of the variance. **b, c** PLS-DA score plots representing the distribution of samples with component 1 vs component 2 (**b**), and component 1 vs component 3 (**c**). All infected recipient (R) fish clustered separated from control (C) fish. In addition, R fish with high intensity of infection (H) were more separated from C than R with low (L) and medium (M) infection levels. R fish with the highest infection levels are included in the rectangle. The contribution of the different metabolites to the group separation was determined by variable importance in projection (VIP) measurements after three components. **d** List of the metabolites increased (in red) or decreased (in green) during the infection, and their VIP (variable importance in projection) scores





and later on perturbs the TJ proteins to stimulate water and ion secretion [46]. The diarrhoea induced by the intracellular parasite *Cryptosporidium parvum* is due to an increased paracellular permeability associated with decreased levels of several TJ and AJ proteins *in vitro* and also to the downregulation of genes related to TJs and AJs in response to the infection in *ex vivo* and *in vivo* mouse models [47]. Similarly, the reduction in the intestinal barrier function induced by *Giardia duodenalis* implicates disruptions of several TJ proteins [48].

The observed changes in permeability and Rt in the current fish-parasite model could also be due to the decreased presence of some TJ proteins in GSB parasitized intestines, as shown by IHC. TJs in enterocytes separate the intestinal lumen from the under-lying tissues, regulating the movement of ions and macromolecules, and thus maintaining the homeostasis. Claudins are essential components of TJs regulating paracellular solute transport. Claudins can alter or be altered by a number of signalling molecules/pathways. Abnormal expression and/or mislocalization of claudins are associated with many human and animal diseases [49]. Some studies have shown that the paracellular resistance of CLDN3-transfected monolayers was strongly elevated, causing an increase in transepithelial resistance. CLDN3 altered the TJ meshwork and sealed the paracellular pathway against the passage of small ions [50]. The downregulation of claudins at protein and gene level can be induced by different factors, including inflammation [51]. In teleost fish, at least 63 claudin genes have been described, but very little is known about their role in the GI tract physiology [52]. The abundance of claudins can

vary spatially along the GI tract of teleosts and it progressively “tightens”, from the anterior to posterior part, thus preventing leakage of water back into the gut lumen [52–54]. Different dietary interventions have variable effects on fish intestinal TJs. Vitamin A deficiency decreased the mRNA levels of TJ complexes (several *cldn*s and *tjp1*) in grass carp (*Ctenopharyngodon idella*) [55], dietary isoleucine decreased the expression of several *cldn*s in Jian carp (*Cyprinus carpio* var. Jian) [56], dietary deoxynivalenol (a mycotoxin) also decreased the relative expression of markers for three TJ proteins in Atlantic salmon (*Salmo salar*) intestine [57], and some plant proteins induced significant alterations of the TJ signalling pathway in this same species [11]. By contrast, dietary stachyose increased the gene expression of *cldn3* and *tjp1* in turbot (*Scophthalmus maximus*) [58], and an olive oil bioactive extract increased *cldn3* expression in GSB [59], whereas some dietary interventions did not change the expression of *tjp1* in GSB [60].

The deleterious effects of pathogens on intestinal TJ integrity is poorly featured in fish, and initially determined by morphological changes [61–63]. More recently, the effect of pathogens on *cldn* transcript abundance in the intestine following viral and bacterial experimental infections has also been reported but with opposite trends. Claudin genes were significantly downregulated in the intestine of catfish (*Ictalurus punctatus*) at three hours post-infection with *Edwardsiella ictaluri*, the bacterial agent causing enteric septicemia [64]. Similarly, the expression of *tjp1* and several *cldn*s was decreased in grass carp 72 hours after *Aeromonas hydrophila* infection [14]. On the other hand, following cyprinid herpesvirus

3 (CyHV-3) infection, mRNA encoding for several *cldns* significantly increased in the intestine of common carp (*Cyprinus carpio*) in conjunction with an upregulation of genes involved in the inflammatory response. It was proposed that alterations in *cldns* abundance may contribute to mechanisms that compensate for a possible disruption of proteins by nitric oxide produced during an immune response of the host to virus-induced tissue damage [65]. No information is available on the effect of fish parasites in intestinal TJs.

In the present study we did not observe a strong change in the intestinal immunolabelling of CDH1; however, its gene expression was significantly downregulated in severely *E. leei*-infected GSB [66]. Classical cadherins, such as E-cadherin (CDH1), are the major transmembrane proteins of AJ and initiate intercellular contacts through trans-pairing between cadherins on opposing cells. Formation of the AJ leads to assembly of the TJ, but E-cadherin is not required to maintain TJ organization [67]. Alterations of E-cadherin are associated with a variety of gastrointestinal disorders. In mammals, intestinal E-cadherin downregulation is usually observed in diseases characterized by high levels of pro-inflammatory molecules, such as inflammatory bowel disease [68, 69]. In fish, E-cadherin gene expression was modulated in the intestine of Atlantic salmon in response to an experimental diet that affected intestinal fluid permeability [44]. In previous studies in GSB, the intestinal gene expression of E-cadherin was also found to be modulated by some dietary interventions. In particular, it was significantly upregulated in GSB fed a diet low in fish meal and fish oil, and it was restored when sodium butyrate was added [33]. However, no changes were detected when fed with Next Enhance[®]150 [54] or with olive oil bioactive compounds [59], and a lower expression was found in the anterior intestine of fish fed DICOSAN or probiotics [70].

In any case, we cannot reject that the changes found in the intestinal barrier integrity could also be due to enterocyte apoptosis and necrosis or to the inflammatory response induced by the parasite, which have been described as acute/chronic in enteromyxosis [15, 71], or to changes in the intestinal mucus layer. In fact, *E. leei*-parasitized GSB have altered glycoprotein profile of the secreted intestinal mucus, bacterial adhesion to large-sized mucus glycoproteins is decreased [72], and important changes in goblet cell composition and distribution and intestinal mucin expression are found [73, 74]. These changes in the intestinal mucus can have a clear effect on the gut barrier, as epithelial TJs and the mucus layer cooperate to form a highly integrated barrier system that together limit access of luminal contents to the body. The capacity of the mucus to prevent abrasion and trap

bacteria represents the first line of defence, while the paracellular TJ barrier prevents leakage of bacterial antigens from the lumen into the body [3].

Altered permeability may lead to impaired digestive functions and reduced fish growth [75], and arrested growth is one of the disease signs of this enteritis [76, 77]. In the present study, this was also evidenced by the differences in weight between R and C fish at the end of all trials. The loss of barrier function can also potentiate systemic absorption of pathogens and toxic molecules which has been shown to be associated with intestinal inflammation in mammals and fish [78, 79].

The untargeted metabolomics study of the serum showed significant changes in the profile of parasitized fish and the PLS-DA clearly separated parasitized fish from control ones into different clusters, confirming the stability and reproducibility of the LC-MS analysis. In previous studies, we have shown that this approach can detect differences in dietary interventions and the nutritional status of GSB [25, 26]. Metabolomics have been applied recently in several areas of aquaculture [27], including infectious fish diseases [24]. However, its application in fish parasitic diseases is very scarce, and only done thus far in naturally infected fish. In one of the few studies, in *Coilia nasus*, from the 391 annotated compounds, 65 metabolites were significantly regulated in Anisakid-infected groups, and the multivariate analyses of the serum metabolite profiles showed good separation between infected and non-infected samples [80], as in the present study. In a GC/MS study of a very similar enteric myxozoan disease, the PLS-DA of 53 metabolites showed three distinct groups according to their parasite load [81]. In *E. leei*-infected sera, the regulated metabolites were involved mainly in amino acid catabolism, fatty acid oxidation, nucleoside, lysophospholipid, vitamin and polyphenol metabolism. Similarly, in the above mentioned cases, the main pathways affected by the parasitic infection were amino acids and fatty acids [81] and amino acids, nucleotide derivatives, phospholipids, and immune-related metabolites [80].

In the present GSB metabolomic profile, some of the regulated compounds deserve special attention. Interestingly, two vitamins, biotin (vitamin B7) and pantothenic acid (vitamin B5) were more downregulated in severely infected GSB than in slightly infected animals. Biotin was also downregulated in short-term fasted fish [25], and we consider that the lowered levels of these vitamins could be due to the reduced nutrient availability reflecting the poor nutritional status of parasitized fish. Further studies are needed to determine the specific role of these vitamins on the pathophysiology of enteromyxosis and its possible therapeutic use, since several studies have shown the role of the intestinal biotin uptake system in the

maintenance of mucosal integrity [82]. Biotin deficiency also induces active intestinal inflammation in mice similar to that observed in ulcerative colitis [82, 83] and leads to an array of pathological conditions in humans, including inflammatory bowel disease [84]. In addition, under biotin-deficient conditions, innate immune system cells produce increased levels of pro-inflammatory cytokines and Th1- and Th17-mediated proinflammatory responses in human CD4+ T lymphocytes [85]. Furthermore, both deficiency and excess of dietary pantothenic acid down-regulate several *clnns*, *occludin* and *tjp1* mRNA levels in all intestinal segments of grass carp [86], and dietary deficiency of another vitamin (vitamin A) also impaired physical barrier functions associated with impaired antioxidant capacity, aggravated cell apoptosis and disrupted TJ complexes in the intestine of grass carp [55]. In contrast, another vitamin related compound, para-aminobenzoic acid (PABA), was increased in parasitized fish. PABA is an intermediate in the synthesis of the vitamin folate by bacteria, plants and fungi. Many bacteria, including those found in the human intestinal tract generate PABA. Humans lack the enzymes to convert PABA to folate, so require folate from dietary sources, such as green leafy vegetables, and rely on the intestinal microbiota. This also happens in fish, as Duncan et al. [87] demonstrated that intestinal microorganisms are a significant source of folic acid for channel catfish, and Kashiwada et al. [88] isolated folic acid-synthesizing bacteria from the intestine of common carp. Therefore, it is tempting to suggest that the intestinal alteration induced by the parasite could also induce changes in the intestinal microbiota of our fish, and therefore changes in the microorganisms capable of converting PABA to folate. Further research on microbial changes in the intestine of parasitized fish will help elucidate these changes.

Several carnitine-related compounds and two γ -glutamyl dipeptides were strongly increased in parasitized GSB (again, more in severely infected than in slightly infected animals). High circulating concentrations of γ -Glu-(Leu/Val/Ile) and five sub-products of L-carnitine were also found in the serum of fasted GSB [25]. These authors suggested that the increased levels of γ -glutamyl dipeptides were due to changes in the Meister's glutamyl cycle, which has a key role in the recovery and delivery of cysteine in the body and transport of amino acids across cell membranes [89]. One of the key actors of this cycle is γ -glutamyl transferase (GGT), an enzyme that generates γ -glutamyl dipeptides by transferring the γ -glutamyl moiety from glutathione (GSH) to amino acids. Expression of GGT is essential in maintaining the cysteine levels in the body. Induction of GGT expression in response to redox stress provides the cell with access to additional cysteine, which

becomes rate-limiting for intracellular GSH synthesis. Increased levels of plasma GGT were found in mice with viral infection [90], and in the liver and muscle of GSB fed diets with high levels of plant proteins [91]. This cycle could also be altered by changes in GSH. In fact, several glutamyl dipeptides have been used as biomarkers of human liver diseases because in healthy individuals the level of hepatic GSH is high and a small amount of GSH is biosynthesized. However, in patients with liver diseases, GSH is consumed to neutralize the generated ROS, which in turn leads to glutamyl cysteine synthetase (GCS) activation, resulting in the biosynthesis of GSH together with glutamyl dipeptides [92]. We can only speculate about this activation in the present study, but it is tempting to suggest it could also happen, as ROS are increased in parasitized GSB and a counteracting role of ROS was hypothesized when downregulated gene expression of *gpx-1* was found in the head kidney and intestine of parasitized GSB [76].

The increased levels of carnitine-related compounds in parasitized GSB are interpreted as increased mobilization of body fat stores, common in fasted individuals, exemplified by the loss of body weight in parasitized fish. Carnitine is actively transported into the cytosol to participate in the shuttling of activated long chain fatty acids into the mitochondria where β -oxidation takes place. During fasting and malnutrition, metabolic adaptations are triggered by PPAR α (peroxisome proliferator-activated receptor alpha) to minimize the use of protein and carbohydrates as fuel to allow survival during long periods of energy deprivation and lipolysis pathways are engaged instead. Carnitine plays a critical role in energy balance across cell membranes and in energy metabolism of tissues that derive much of their energy from fatty acid oxidation such as cardiac and skeletal muscles [93]. In our case, the long-term infection also engaged protein catabolism in parasitized GSB, since different metabolites related to amino acid catabolism were highly increased, as is the case for oxoadipic acid (more than 4700% in highly parasitized fish), which is a key catabolite of the essential amino acids tryptophan and lysine.

The two selected metabolites (creatinine and inosine) emerged as good markers to differentiate C and R fish. Creatinine was significantly increased in proportion to the degree of infection in parasitized GSB, and also when the ELISA was performed in additional samples. Creatinine is a nitrogenous organic acid, made from arginine, glycine and methionine. It is a key component of phosphocreatine, which works as a store for high energy phosphate in the muscle, as ATP is produced at the expense of ADP *via* the phosphocreatine shuttle and creatine kinase in active muscles. It is generally accepted that creatinine increases as muscle protein is broken down and creatinine

levels are maintained by diet and endogenous synthesis. In fact, in humans, creatine amounts to more than 20% of the dietary intake of arginine [94]. The same happened for inosine, but with the opposite trend. Inosine, an endogenous purine nucleoside formed by the degradation of adenosine, is produced and released into the extracellular space during normal cell metabolism. Adenosine has a short half-life, whereas inosine has a much longer *in vivo* half-life. It was originally thought to have no biological effects. However, recent studies demonstrate that inosine has potent immunomodulatory and neuroprotective effects and increased inosine levels are present in various inflammatory states and heart conditions [95, 96]. We can only speculate about the meaning of the low levels found in parasitized GSB, which point to a dysfunction of purine metabolism. The first hypothesis is a decreased catabolism of adenosine, in an effort to maintain the fish energy homeostasis, due to the involvement of adenosine

in ATP/ADP balance. The second would be the uptake of inosine by the parasite, as shown for parasitic protozoa that lack the enzymes required for *de novo* synthesis of purines and are therefore reliant upon the salvage of these compounds from the external environment [97]. Unfortunately, we do not have such information for *E. leei*, but recent genomic data of another myxozoan, *Thelohanellus kitauei*, seems to indicate that this parasite has lost the ATP-expensive pathways for *de novo* biosynthesis of inosine 50-phosphate and uridine 50-phosphate. Therefore, it must rely on salvage pathways as well [98]. If this is the case of *E. leei*, the possible therapeutic use of inosine against enteromyxosis is worth further investigation, since dietary inosine supplementation reduced the oxidative stress and improved intestinal health condition and immune response in several fish species [99, 100]. In fact, treatment with inosine compounds is currently being used for some human viral infections [101].

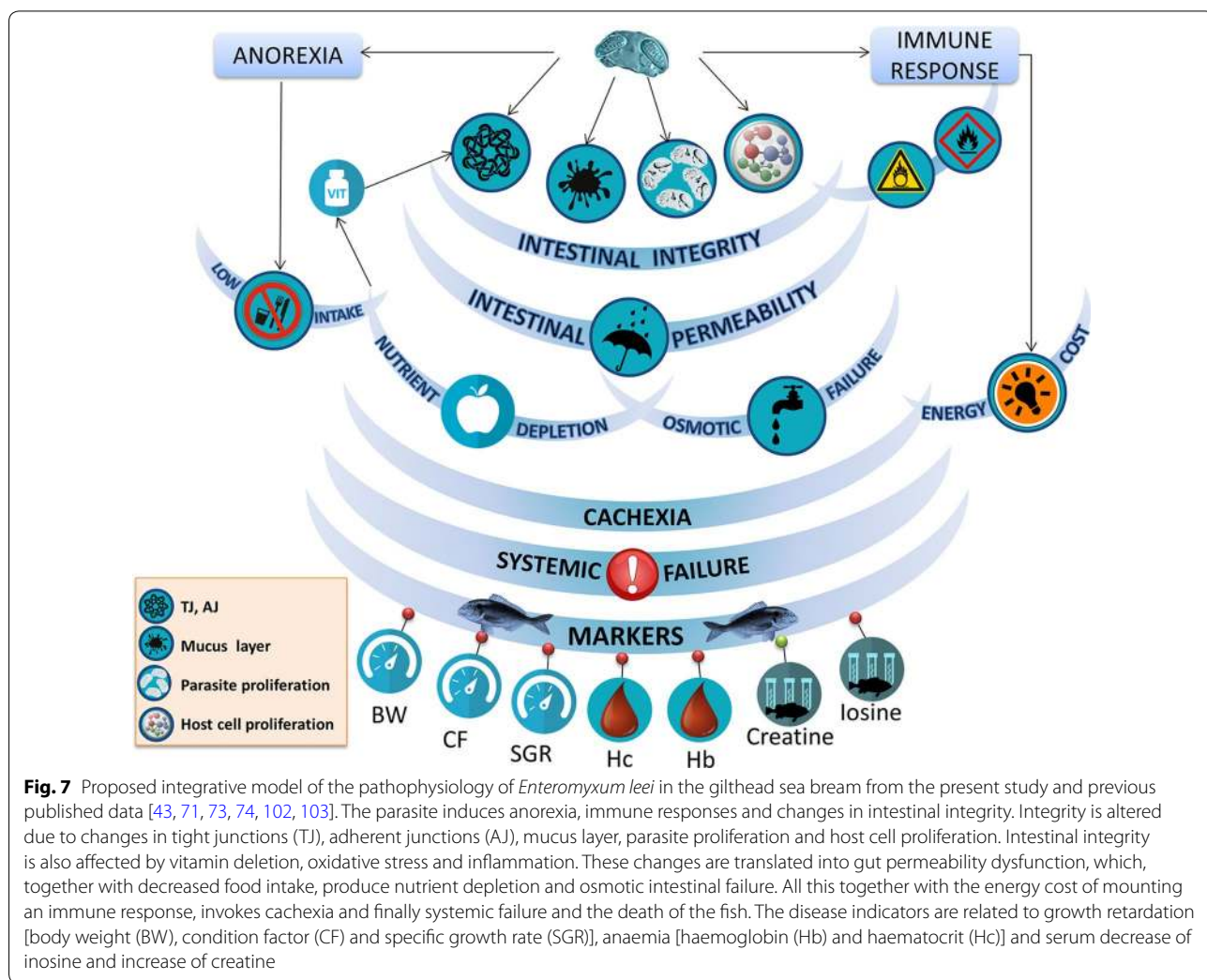


Fig. 7 Proposed integrative model of the pathophysiology of *Enteromyxum leei* in the gilthead sea bream from the present study and previous published data [43, 71, 73, 74, 102, 103]. The parasite induces anorexia, immune responses and changes in intestinal integrity. Integrity is altered due to changes in tight junctions (TJ), adherent junctions (AJ), mucus layer, parasite proliferation and host cell proliferation. Intestinal integrity is also affected by vitamin deletion, oxidative stress and inflammation. These changes are translated into gut permeability dysfunction, which, together with decreased food intake, produce nutrient depletion and osmotic intestinal failure. All this together with the energy cost of mounting an immune response, invokes cachexia and finally systemic failure and the death of the fish. The disease indicators are related to growth retardation [body weight (BW), condition factor (CF) and specific growth rate (SGR)], anaemia [haemoglobin (Hb) and haematocrit (Hc)] and serum decrease of inosine and increase of creatine

Conclusions

To our knowledge, our results provide the first functional evidence of the disruption of the gut integrity by the fish parasite *Enteromyxum leei*. The clear decrease of the immunolabelling of several tight junction proteins along the intestine of parasitized fish leads to changes in the intercellular sealing, the selective diffusion barrier between epithelial cells and the prevention of the free passage of molecules and ions across the paracellular pathway. This was substantiated by the increased gut paracellular uptake and the decreased transepithelial resistance in infected animals, which showed a diarrheic profile. We have also demonstrated that parasitized fish have a distinct serum metabolomic profile, and that two metabolites (creatine and inosine) are good markers to differentiate parasitized and non-parasitized fish. The depletion of several metabolites involved in vitamin pathways opens the door to find future new palliative treatments. These results allow drawing a better picture of the complex interplay of the different factors involved in the pathophysiology of this disease, which are summarized in Fig. 7. The disruption of the intestinal integrity contributes to nutrient malabsorption, osmoregulatory failure and cachexia that eventually contribute to systemic organ failure.

Supplementary information

Supplementary information accompanies this paper at <https://doi.org/10.1186/s13071-019-3746-7>.

Additional file 1: Figure S1. Orthogonal PLS-DA S-Plot of injected serum samples. Ions enhanced by enteritis are at the top-right and those decreased by enteritis are at the bottom-left. In red, ions of the selected compounds that were elucidated.

Abbreviations

AI: anterior intestinal segment; AJ: adherens junction; C: control group; CDH1: E-cadherin; CLDN-3: claudin-3; dpe: days post-exposure; dpi: days post-intubation; FITC: fluorescein isothiocyanate; GC/MS: gas chromatography/mass spectrometry; GCS: glutamyl cysteine synthetase; GGT: γ -glutamyl transferase; GI: gastrointestinal; GSB: gilthead sea bream; GSH: glutathione; HILIC: hydrophilic interaction liquid chromatography; IHC: immunohistochemistry; Isc: short-circuit current; LC-MS: liquid chromatography-mass spectrometry; NL: non-lethal sampling; PABA: para-aminobenzoic acid; PI: posterior intestinal segment; PLS-DA: partial least-squares discriminant analysis; R: recipient group; ROS: reactive oxygen species; RP: reverse phase chromatography; Rt: epithelial resistance; TJs: tight junctions; TJP1: tight junction protein 1; VIP: variable importance in projection.

Acknowledgements

The authors thank J. Monfort and L. Rodríguez for histological processing, R. del Pozo for technical assistance with molecular diagnosis and fish husbandry, and X. Pérez-Sitjà for the design of the graphical abstract. This work has been conducted within the framework of the Research Unit of Marine Ecotoxicology (IATS-CSIC/IUPA-UJI).

Authors' contributions

Conceptualization: ASB and JPS. Data curation: JCG, JPS, RGS and JVS. Formal analysis: IE, MCP, RGS, JVS and JAMS. Investigation: RGS, IE, MCP, JCG, APS, JF, ASB and JPS. Project administration: ASB and JPS. Resources: FH, JPS and ASB.

Funding acquisition: ASB, JPS and JF. Supervision: ASB and JPS. Visualisation: IE, MCP and ASB. Writing original draft: ASB, MCP and JPS. Writing review and editing: all authors. All authors read and approved the final manuscript.

Funding

This work has been carried out with financial support from the European Union under grant projects ParaFishControl (H2020-634429) to ASB and Aquacelx²⁰²⁰ (652831, TNA AE10004-INTEBREAM) to JF and JPS, and from the Spanish MINECO under AGL2013-48560-R project to ASB and JPS. APS was contracted under the ParaFishControl project, MCP under CSIC PIE project no. 201740E013 and IE under APOSTD/2016/037 grant by the "Generalitat Valenciana". Centre for Marine Sciences (CCMAR) is supported by the Portuguese Foundation for Science and Technology (FCT) through project UID/Multi/04326/2019. This publication reflects the views only of the authors, and the European Commission cannot be held responsible for any use which may be made of the information.

Availability of data and materials

All data generated by this study are included in the article and its additional file. Metabolomics data have been uploaded as MetaboLights study reference MTBLS1194 and are available at <http://www.ebi.ac.uk/metabolights/MTBLS1194>. MetaboLights is an open access repository for metabolomics studies [104].

Ethics approval and consent to participate

All experimental protocols involving fish were approved by the Ethics and Animal Welfare Committee of IATS, CSIC and Generalitat Valenciana. They were carried out in a registered installation facility (code ES120330001055) in accordance with the principles published in the European animal directive (2010/63/EU) and Spanish laws (Royal Decree RD53/2013) for the protection of animals used in scientific experiments. For infection trials and lethal samplings, all efforts were made to minimize the suffering of animals.

Consent for publication

Not applicable.

Competing interests

The authors declare that they have no competing interests.

Author details

¹ Fish Pathology Group, Instituto de Acuicultura Torre de la Sal (IATS-CSIC), 12595 Ribera de Cabanes, Castellón, Spain. ² Associated Unit of Marine Ecotoxicology (IATS-IUPA), Castellón, Spain. ³ Research Institute for Pesticides and Water (IUPA), University Jaume I, Avda. Vicent Sos Baynat, s/n. Campus del Riu Sec, 12071 Castellón, Spain. ⁴ Nutrigenomics and Fish Endocrinology Group, Instituto de Acuicultura Torre de la Sal (IATS-CSIC), 12595 Ribera de Cabanes, Castellón, Spain. ⁵ Department of Biology, Faculty of Marine and Environmental Sciences, Instituto Universitario de Investigación Marina (INMAR), Campus Universitario de Puerto Real, University of Cádiz, 11510 Cádiz, Spain. ⁶ Comparative Endocrinology and Integrative Biology, CCMar, University of Algarve, Campus de Gambelas, 8005-139 Faro, Portugal.

Received: 31 July 2019 Accepted: 9 October 2019

Published online: 16 October 2019

References

- Halliez MCM, Buret AG. Gastrointestinal parasites and the neural control of gut functions. *Front Cell Neurosci.* 2015;9:452.
- Yun CH, Lillehoj HS, Lillehoj EP. Intestinal immune responses to coccidiosis. *Dev Comp Immunol.* 2000;24:303–24.
- Capaldo CT, Powell DN, Kalman D. Layered defense: how mucus and tight junctions seal the intestinal barrier. *J Mol Med.* 2017;95:927–34.
- Olivera-Villagomez D, Van Kaer L. Intestinal intraepithelial lymphocytes: sentinels of the mucosal barrier. *Trends Immunol.* 2018;39:264–75.
- Chelakkot C, Ghim J, Ryu SH. Mechanisms regulating intestinal barrier integrity and its pathological implications. *Exp Mol Med.* 2018;50:103.
- Brandl K, Schnabl B. Is intestinal inflammation linking dysbiosis to gut barrier dysfunction during liver disease? *Expert Rev Gastroenterol Hepatol.* 2015;9:1069–76.

7. Cain K, Swan C. Barrier function and immunology. In: Grosell M, Farrell AP, Brauner CJ, editors. The multifunctional gut of fish. San Diego: Academic Press; 2011. p. 112–65.
8. Laporte J, Trushenski J. Production performance, stress tolerance and intestinal integrity of sunshine bass fed increasing levels of soybean meal. *J Anim Physiol Anim Nutr*. 2012;96:513–26.
9. Couto A, Kortner TM, Penn M, Bakke AM, Krogdahl Å, Oliva-Teles A. Effects of dietary phytosterols and soy saponins on growth, feed utilization efficiency and intestinal integrity of gilthead sea bream (*Sparus aurata*) juveniles. *Aquaculture*. 2014;432:295–303.
10. Torrecillas S, Montero D, Izquierdo M. Improved health and growth of fish fed mannan oligosaccharides: potential mode of action. *Fish Shellfish Immunol*. 2014;36:525–44.
11. Krol E, Douglas A, Tocher DR, Crampton VO, Speakman JR, Secombes CJ, et al. Differential responses of the gut transcriptome to plant protein diets in farmed Atlantic salmon. *BMC Genomics*. 2016;17:156.
12. Maricchiolo G, Caccamo L, Mancuso M, Cusimano GM, Gai F, Genovese M, et al. *Saccharomyces cerevisiae* var. *boulardii* preserves the integrity of intestinal mucosa in gilthead seabream, *Sparus aurata* subjected to a bacterial challenge with *Vibrio anguillarum*. *Aquac Res*. 2017;48:725–8.
13. Estruch G, Collado MC, Monge-Ortiz R, Tomás-Vidal A, Jover-Cerdá M, Peñaranda DS, et al. Long-term feeding with high plant protein based diets in gilthead seabream (*Sparus aurata*, L.) leads to changes in the inflammatory and immune related gene expression at intestinal level. *BMC Vet Res*. 2018;14:302.
14. Kong W-G, Li S-S, Chen X-X, Huang Y-Q, Tang Y, Wu Z-X. A study of the damage of the intestinal mucosa barrier structure and function of *Ctenopharyngodon idella* with *Aeromonas hydrophila*. *Fish Physiol Biochem*. 2017;43:1223–35.
15. Sitjà-Bobadilla A, Palenzuela O. Myxozoan biology and ecology. In: UNESCO-EOLSS Joint Committee, editors. Fisheries and aquaculture. Encyclopedia of Life Support Systems (EOLSS). Paris: Eolss Publishers; 2013. <http://www.eolss.net>.
16. Sitjà-Bobadilla A, Palenzuela O. *Enteromyxum* species. In: Woo P, Buchmann K, editors. Fish parasites: pathobiology and protection. London: CAB; 2012. p. 163–76.
17. Cuadrado M, Marqués A, Diamant A, Sitjà-Bobadilla A, Palenzuela O, Álvarez-Pellitero P, et al. Ultrastructure of *Enteromyxum leei* (Diamant, Lom, & Dykova, 1994) (Myxozoa), an enteric parasite infecting gilthead sea bream (*Sparus aurata*) and sharpnose sea bream (*Diplodus puntazzo*). *J Eukaryot Microbiol*. 2008;55:178–84.
18. Fleurance R, Sauvegrain C, Marques A, Le Breton A, Guereaud C, Chérel Y, et al. Histopathological changes caused by *Enteromyxum leei* infection in farmed sea bream *Sparus aurata*. *Dis Aquat Organ*. 2008;79:219–28.
19. Cuadrado-Lafoz M. Enteromixosi produïda per *Enteromyxum leei* (Diamant, Lom i Dyková, 1994) en espèrdis d'interès comercial del Mediterrani. PhD Thesis, Universitat Autònoma de Barcelona, Spain; 2010.
20. Giorgini E, Randazzo B, Gioacchini G, Cardinaletti G, Vaccari L, Tibaldi E, et al. New insights on the macromolecular building of rainbow trout (*O. mykiss*) intestine: FTIR imaging and histological correlative study. *Aquaculture*. 2018;497:1–9.
21. Goossens E, Debyser G, Callens C, De Gussem M, Dedeurwaerder A, Devreese B, et al. Elevated faecal ovotransferrin concentrations are indicative for intestinal barrier failure in broiler chickens. *Vet Res*. 2018;49:51.
22. Wells JM, Brummer RJ, Derrien M, MacDonald TT, Troost F, Cani PD, et al. Homeostasis of the gut barrier and potential biomarkers. *Am J Physiol Gastrointest Liver Physiol*. 2017;312:G171–93.
23. Helms JB, Kaloyanova DV, Strating JRP, van Hellemond JJ, van der Schaaf HM, Tielens AGM, et al. Targeting of the hydrophobic metabolome by pathogens. *Traffic*. 2015;16:439–60.
24. Low C-F, Rozaini MZH, Musa N, Syarul Nataqain B. Current knowledge of metabolomic approach in infectious fish disease studies. *J Fish Dis*. 2017;40:1267–77.
25. Gil-Solsona R, Nàcher-Mestre J, Lacalle-Bergeron L, Sancho JV, Calduch-Giner JA, Hernández F, et al. Untargeted metabolomics approach for unraveling robust biomarkers of nutritional status in fasted gilthead sea bream (*Sparus aurata*). *PeerJ*. 2017;5:e2920.
26. Gil-Solsona R, Calduch-Giner JA, Nàcher-Mestre J, Lacalle-Bergeron L, Sancho JV, Hernández F, et al. Contributions of MS metabolomics to gilthead sea bream (*Sparus aurata*) nutrition. Serum fingerprinting of fish fed low fish meal and fish oil diets. *Aquaculture*. 2019;498:503–12.
27. Alfaro AC, Young T. Showcasing metabolomic applications in aquaculture: a review. *Rev Aquac*. 2018;10:135–52.
28. Picard-Sánchez A, Estensoro I, del Pozo R, Piazzon MC, Palenzuela O, Sitjà-Bobadilla A. Acquired protective immune response in a fish-myxozoan model encompasses specific antibodies and inflammation resolution. *Fish Shellfish Immunol*. 2019;90:349–62.
29. Sitjà-Bobadilla A, Diamant A, Palenzuela O, Álvarez-Pellitero P. Effect of host factors and experimental conditions on the horizontal transmission of *Enteromyxum leei* (Myxozoa) to gilthead sea bream, *Sparus aurata* L., and European sea bass, *Dicentrarchus labrax* (L.). *J Fish Dis*. 2007;30:243–50.
30. Estensoro I, Redondo MJ, Álvarez-Pellitero P, Sitjà-Bobadilla A. Novel horizontal transmission route for *Enteromyxum leei* (Myxozoa) by anal intubation of gilthead sea bream *Sparus aurata*. *Dis Aquat Organ*. 2010;92:51–8.
31. Ronza P, Villamarín A, Méndez L, Pardo BG, Bermúdez R, Quiroga MI. Immunohistochemical expression of E-cadherin in different tissues of the teleost fish *Scophthalmus maximus*. *Aquaculture*. 2019;501:465–72.
32. Carvalho ESM, Gregorio SF, Power DM, Canario AVM, Fuentes J. Water absorption and bicarbonate secretion in the intestine of the sea bream are regulated by transmembrane and soluble adenylyl cyclase stimulation. *J Comp Physiol B*. 2012;182:1069–80.
33. Estensoro I, Ballester-Lozano G, Benedito-Palos L, Grammes F, Martos-Sitcha JA, Mydland L-T, et al. Dietary butyrate helps to restore the intestinal status of a marine teleost (*Sparus aurata*) fed extreme diets low in fish meal and fish oil. *PLoS ONE*. 2016;11:e0166564.
34. Li H, Ma M-L, Luo S, Zhang R-M, Han P, Hu W. Metabolic responses to ethanol in *Saccharomyces cerevisiae* using a gas chromatography tandem mass spectrometry-based metabolomics approach. *Int J Biochem Cell Biol*. 2012;44:1087–96.
35. Kieffer DA, Piccolo BD, Vaziri ND, Liu S, Lau WL, Khazaeli M, et al. Resistant starch alters gut microbiome and metabolomic profiles concurrent with amelioration of chronic kidney disease in rats. *Am J Physiol Renal Physiol*. 2016;310:F857–71.
36. Turner JR. Intestinal mucosal barrier function in health and disease. *Nat Rev Immunol*. 2009;9:799–809.
37. Srinivasan B, Kolli AR, Esch MB, Abaci HE, Shuler ML, Hickman JJ. TEER measurement techniques for *in vitro* barrier model systems. *J Lab Autom*. 2015;20:107–26.
38. Yeste J, Illa X, Alvarez M, Villa R. Engineering and monitoring cellular barrier models. *J Biol Eng*. 2018;12:18.
39. Schug H, Begnaud F, Debonneville C, Berthaud F, Gimeno S, Schirmer K. TransFER: a new device to measure the transfer of volatile and hydrophobic organic chemicals across an *in vitro* intestinal fish cell barrier. *Anal Methods*. 2018;10:4394–403.
40. Liu Y, Chen Z, Dai J, Yang P, Xu W, Ai Q, et al. Sodium butyrate supplementation in high-soybean meal diets for turbot (*Scophthalmus maximus* L.): effects on inflammatory status, mucosal barriers and microbiota in the intestine. *Fish Shellfish Immunol*. 2019;88:65–75.
41. Mosberian-Tanha P, Overland M, Landsverk T, Reveco FE, Schrama JW, Roem AJ, et al. Bacterial translocation and *in vivo* assessment of intestinal barrier permeability in rainbow trout (*Oncorhynchus mykiss*) with and without soyabean meal-induced inflammation. *J Nutr Sci*. 2016;5:e26.
42. Sundh H, Olsen R-E, Fridell F, Gadan K, Evensen O, Glette J, et al. The effect of hyperoxygenation and reduced flow in fresh water and subsequent infectious pancreatic necrosis virus challenge in sea water, on the intestinal barrier integrity in Atlantic salmon, *Salmo salar* L. *J Fish Dis*. 2009;32:687–98.
43. Ishimatsu A, Hayashi M, Nakane M, Sameshima M. Pathophysiology of cultured tiger puffer *Takifugu rubripes* suffering from the Myxosporean emaciation disease. *Fish Pathol*. 2007;42:211–7.
44. Hu H, Kortner TM, Gajardo K, Chikwati E, Tinsley J, Krogdahl A. Intestinal fluid permeability in Atlantic salmon (*Salmo salar* L.) is affected by dietary protein source. *PLoS ONE*. 2016;11:e0167515.
45. Gu M, Jia Q, Zhang Z, Bai N, Xu X, Xu B. Soya-saponins induce intestinal inflammation and barrier dysfunction in juvenile turbot (*Scophthalmus maximus*). *Fish Shellfish Immunol*. 2018;77:264–72.

46. Cornick S, Chadee K. *Entamoeba histolytica*: host parasite interactions at the colonic epithelium. *Tissue Barriers*. 2017;5:e1283386.
47. Kumar A, Chatterjee I, Anbazhagan AN, Jayawardena D, Priyamvada S, Alrefai WA, et al. *Cryptosporidium parvum* disrupts intestinal epithelial barrier function via altering expression of key tight junction and adherens junction proteins. *Cell Microbiol*. 2018;20:e12830.
48. Buret AG, Amat CB, Manko A, Beatty JK, Halliez MCM, Bhargava A, et al. *Giardia duodenalis*: new research developments in pathophysiology, pathogenesis, and virulence factors. *Curr Trop Med Reports*. 2015;2:110–8.
49. Lu Z, Ding L, Lu Q, Chen Y-H. Claudins in intestines: distribution and functional significance in health and diseases. *Tissue Barriers*. 2013;1:e24978.
50. Milatz S, Krug SM, Rosenthal R, Gunzel D, Muller D, Schulzke J-D, et al. Claudin-3 acts as a sealing component of the tight junction for ions of either charge and uncharged solutes. *Biochim Biophys Acta*. 2010;1798:2048–57.
51. Garcia-Hernandez V, Quiros M, Nusrat A. Intestinal epithelial claudins: expression and regulation in homeostasis and inflammation. *Ann NY Acad Sci*. 2017;1397:66–79.
52. Kolosov D, Bui P, Chasiotis H, Kelly SP. Claudins in teleost fishes. *Tissue Barriers*. 2013;1:e25391.
53. Tipsmark CK, Sorensen KJ, Hulgard K, Madsen SS. Claudin-15 and -25b expression in the intestinal tract of Atlantic salmon in response to seawater acclimation, smoltification and hormone treatment. *Comp Biochem Physiol A Mol Integr Physiol*. 2010;155:361–70.
54. Pérez-Sánchez J, Benedito-Palos L, Estensoro I, Petropoulos Y, Calduch-Giner JA, Browdy CL, et al. Effects of dietary NEXT ENHANCE®150 on growth performance and expression of immune and intestinal integrity related genes in gilthead sea bream (*Sparus aurata* L.). *Fish Shellfish Immunol*. 2015;44:117–28.
55. Jiang W-D, Zhou X-Q, Zhang L, Liu Y, Wu P, Jiang J, et al. Vitamin A deficiency impairs intestinal physical barrier function of fish. *Fish Shellfish Immunol*. 2019;87:546–58.
56. Zhao J, Feng L, Liu Y, Jiang W, Wu P, Jiang J, et al. Effect of dietary isoleucine on the immunity, antioxidant status, tight junctions and microflora in the intestine of juvenile Jian carp (*Cyprinus carpio* var. Jian). *Fish Shellfish Immunol*. 2014;41:663–73.
57. Moldal T, Bernhoft A, Rosenlund G, Kaldhusdal M, Koppang EO. Dietary deoxynivalenol (DON) may impair the epithelial barrier and modulate the cytokine signaling in the intestine of Atlantic salmon (*Salmo salar*). *Toxins*. 2018;10:376.
58. Yang P, Hu H, Liu Y, Li Y, Ai Q, Xu W, et al. Dietary stachyose altered the intestinal microbiota profile and improved the intestinal mucosal barrier function of juvenile turbot, *Scophthalmus maximus* L. *Aquaculture*. 2018;486:98–106.
59. Gisbert E, Andree KB, Quintela JC, Calduch-Giner JA, Ipharraguerre IR, Pérez-Sánchez J. Olive oil bioactive compounds increase body weight, and improve gut health and integrity in gilthead sea bream (*Sparus aurata*). *Br J Nutr*. 2017;117:351–63.
60. Cerezuela R, Meseguer J, Esteban MA. Effects of dietary inulin, *Bacillus subtilis* and microalgae on intestinal gene expression in gilthead sea-bream (*Sparus aurata* L.). *Fish Shellfish Immunol*. 2013;34:843–8.
61. Del-Pozo J, Crumlish M, Turnbull JF, Ferguson HW. Histopathology and ultrastructure of segmented filamentous bacteria-associated rainbow trout gastroenteritis. *Vet Pathol*. 2010;47:220–30.
62. Ringo E, Salinas I, Olsen RE, Nyhaug A, Myklebust R, Mayhew TM. Histological changes in intestine of Atlantic salmon (*Salmo salar* L.) following *in vitro* exposure to pathogenic and probiotic bacterial strains. *Cell Tissue Res*. 2007;328:109–16.
63. Ringo E, Jutfelt F, Kanapathippillai P, Bakken Y, Sundell K, Glette J, et al. Damaging effect of the fish pathogen *Aeromonas salmonicida* ssp. *salmonicida* on intestinal enterocytes of Atlantic salmon (*Salmo salar* L.). *Cell Tissue Res*. 2004;318:305–11.
64. Sun L, Liu S, Bao L, Li Y, Feng J, Liu Z. Claudin multigene family in channel catfish and their expression profiles in response to bacterial infection and hypoxia as revealed by meta-analysis of RNA-Seq datasets. *Comp Biochem Physiol Part D Genomics Proteomics*. 2015;13:60–9.
65. Syakuri H, Adamek M, Brogden G, Rakus KL, Matras M, Irnazarow I, et al. Intestinal barrier of carp (*Cyprinus carpio* L.) during a cyprinid herpesvirus 3-infection: molecular identification and regulation of the mRNA expression of claudin encoding genes. *Fish Shellfish Immunol*. 2013;34:305–14.
66. Ronza P, Estensoro I, Bermúdez R, Losada AP, Pérez-Cordón G, Pardo BG, et al. Cambios en la expresión proteica y génica de la E-cadherina intestinal de dos peces teleosteos inducidos por *Enteromyxum* spp. (Myxozoa). Libro de Actas de la XXVII Reunión de la Sociedad Española de Anatomía Patológica Veterinaria. Córdoba: Ediciones Don Folio; 2016. p. 62.
67. Hartsock A, Nelson WJ. Adherens and tight junctions: structure, function and connections to the actin cytoskeleton. *Biochim Biophys Acta*. 2008;1778:660–9.
68. Arijs I, De Hertogh G, Machiels K, Van Steen K, Lemaire K, Schraenen A, et al. Mucosal gene expression of cell adhesion molecules, chemokines, and chemokine receptors in patients with inflammatory bowel disease before and after infliximab treatment. *Am J Gastroenterol*. 2011;106:748–61.
69. Sanders DSA. Mucosal integrity and barrier function in the pathogenesis of early lesions in Crohn's disease. *J Clin Pathol*. 2005;58:568–72.
70. Simó-Mirabet P, Piazzon MC, Calduch-Giner JA, Ortiz A, Puyalto M, Sitjà-Bobadilla A, et al. Sodium salt medium-chain fatty acids and *Bacillus*-based probiotic strategies to improve growth and intestinal health of gilthead sea bream (*Sparus aurata*). *PeerJ*. 2017;2017:12.
71. Pérez-Cordón G, Estensoro I, Benedito-Palos L, Calduch-Giner JA, Sitjà-Bobadilla A, Pérez-Sánchez J. Interleukin gene expression is strongly modulated at the local level in a fish-parasite model. *Fish Shellfish Immunol*. 2014;37:201–8.
72. Estensoro I, Redondo MJ, Salesa B, Kaushik S, Pérez-Sánchez J, Sitjà-Bobadilla A. Effect of nutrition and *Enteromyxum leei* infection on gilthead sea bream *Sparus aurata* intestinal carbohydrate distribution. *Dis Aquat Organ*. 2012;100:29–42.
73. Estensoro I, Jung-Schroers V, Álvarez-Pellitero P, Steinhagen D, Sitjà-Bobadilla A. Effects of *Enteromyxum leei* (Myxozoa) infection on gilthead sea bream (*Sparus aurata*) (Teleostei) intestinal mucus: glycoprotein profile and bacterial adhesion. *Parasitol Res*. 2013;112:567–76.
74. Pérez-Sánchez J, Estensoro I, Redondo MJ, Calduch-Giner JA, Kaushik S, Sitjà-Bobadilla A. Mucins as diagnostic and prognostic biomarkers in a fish-parasite model: transcriptional and functional analysis. *PLoS ONE*. 2013;8:e65457.
75. Knudsen D, Jutfelt F, Sundh H, Sundell K, Koppe W, Frøkiær H. Dietary soya saponins increase gut permeability and play a key role in the onset of soyabean-induced enteritis in Atlantic salmon (*Salmo salar* L.). *Br J Nutr*. 2008;100:120–9.
76. Sitjà-Bobadilla A, Calduch-Giner J, Saera-Vila A, Palenzuela O, Álvarez-Pellitero P, Pérez-Sánchez J. Chronic exposure to the parasite *Enteromyxum leei* (Myxozoa: Myxosporae) modulates the immune response and the expression of growth, redox and immune relevant genes in gilthead sea bream, *Sparus aurata* L. *Fish Shellfish Immunol*. 2008;24:610–9.
77. Shin SP, Sohn HC, Jin CN, Kang BJ, Lee J. Quantitative investigation of *Enteromyxum leei* (Myxozoa: Myxosporae) infection and relative condition factor in cultured olive flounder *Paralichthys olivaceus* (Temminck and Schlegel). *J Fish Dis*. 2019;42:159–65.
78. Shen L, Su L, Turner JR. Mechanisms and functional implications of intestinal barrier defects. *Dig Dis*. 2009;27:443–9.
79. Jutfelt F. Integrated function and control of the gut. Barrier function of the gut. In: Farrell A, editor. *Encyclopedia of fish physiology*. San Diego: Academic Press; 2011. p. 1322–31.
80. Liu K, Yin D, Shu Y, Dai P, Yang Y, Wu H. Transcriptome and metabolome analyses of *Coilia nasus* in response to Anisakidae parasite infection. *Fish Shellfish Immunol*. 2019;87:235–42.
81. Kodama H, Otani K, Iwasaki T, Takenaka S, Horitani Y, Togase H. Metabolic investigation of pathogenesis of myxosporean emaciation disease of tiger puffer fish *Takifugu rubripes*. *J Fish Dis*. 2014;37:619–27.
82. Sabui S, Bohl JA, Kapadia R, Cogburn K, Ghosal A, Lambrecht NW, et al. Role of the sodium-dependent multivitamin transporter (SMVT) in the maintenance of intestinal mucosal integrity. *Am J Physiol Gastrointest Liver Physiol*. 2016;311:G561–70.
83. Ghosal A, Lambrecht N, Subramanya SB, Kapadia R, Said HM. Conditional knockout of the Slc5a6 gene in mouse intestine impairs biotin absorption. *Am J Physiol Gastrointest Liver Physiol*. 2013;304:G64–71.

84. Fernandez-Banares F, Abad-Lacruz A, Xiol X, Gine JJ, Dolz C, Cabre E, et al. Vitamin status in patients with inflammatory bowel disease. *Am J Gastroenterol.* 1989;84:744–8.
85. Elahi A, Sabui S, Narasappa NN, Agrawal S, Lambrecht NW, Agrawal A, et al. Biotin deficiency induces Th1- and Th17-mediated proinflammatory responses in human CD4(+) T lymphocytes *via* activation of the mTOR signaling pathway. *J Immunol.* 2018;200:2563–70.
86. Li L, Feng L, Jiang W-D, Jiang J, Wu P, Kuang S-Y, et al. Dietary pantothenic acid deficiency and excess depress the growth, intestinal mucosal immune and physical functions by regulating NF-kappaB, TOR, Nrf2 and MLCK signaling pathways in grass carp (*Ctenopharyngodon idella*). *Fish Shellfish Immunol.* 2015;45:399–413.
87. Duncan PL, Lovell RT, Butterworth CEJ, Freeberg LE, Tamura T. Dietary folate requirement determined for channel catfish, *Ictalurus punctatus*. *J Nutr.* 1993;123:1888–97.
88. Kashiwada K, Kanazawa A, Teshima S. Production of folic acid by intestinal bacterial of carp. Studies on the production of B vitamins by intestinal bacteria. Kagoshima: Mem Fac Fish Kagoshima Univ; 1971. p. 185–9.
89. Griffith OW, Bridges RJ, Meister A. Evidence that the gamma-glutamyl cycle functions *in vivo* using intracellular glutathione: effects of amino acids and selective inhibition of enzymes. *Proc Natl Acad Sci USA.* 1978;75:5405–8.
90. Wikoff WR, Kalisak E, Trauger S, Manchester M, Siuzdak G. Response and recovery in the plasma metabolome tracks the acute LCMV-induced immune response. *J Proteome Res.* 2009;8:3578–87.
91. Sitjà-Bobadilla A, Peña-Llopis S, Gómez-Requeni P, Médale F, Kaushik S, Pérez-Sánchez J, et al. Effect of fish meal replacement by plant protein sources on non-specific defense mechanisms and oxidative stress in gilthead sea bream (*Sparus aurata*). *Aquaculture.* 2005;249:387–400.
92. Soga T, Sugimoto M, Honma M, Mori M, Igarashi K, Kashikura K, et al. Serum metabolomics reveals gamma-glutamyl dipeptides as biomarkers for discrimination among different forms of liver disease. *J Hepatol.* 2011;55:896–905.
93. Flanagan JL, Simmons PA, Vehige J, Willcox MD, Garrett Q. Role of carnitine in disease. *Nutr Metab.* 2010;7:30.
94. Brosnan JT, Brosnan ME. Creatine metabolism and the urea cycle. *Mol Genet Metab.* 2010;100(Suppl):S49–52.
95. Hasko G, Sitkovsky MV, Szabo C. Immunomodulatory and neuroprotective effects of inosine. *Trends Pharmacol Sci.* 2004;25:152–7.
96. Farthing DE, Farthing CA, Xi L. Inosine and hypoxanthine as novel biomarkers for cardiac ischemia: from bench to point-of-care. *Exp Biol Med.* 2015;240:821–31.
97. Landfear SM. Nutrient transport and pathogenesis in selected parasitic protozoa. *Eukaryot Cell.* 2011;10:483–93.
98. Yang Y, Xiong J, Zhou Z, Huo F, Miao W, Ran C, et al. The genome of the myxosporean *Thelohanellus kitauei* shows adaptations to nutrient acquisition within its fish host. *Genome Biol Evol.* 2014;6:3182–98.
99. Hossain MS, Koshio S, Ishikawa M, Yokoyama S, Sony NM, Usami M, et al. Inosine supplementation effectively provokes the growth, immune response, oxidative stress resistance and intestinal morphology of juvenile red sea bream, *Pagrus major*. *Aquac Nutr.* 2017;23:952–63.
100. Hossain MS, Koshio S, Ishikawa M, Yokoyama S, Sony NM, Kader MA, et al. Effects of dietary administration of inosine on growth, immune response, oxidative stress and gut morphology of juvenile amberjack, *Seriola dumerili*. *Aquaculture.* 2017;468:534–44.
101. Beran J, Salapova E, Spajdel M. Inosine pranobex is safe and effective for the treatment of subjects with confirmed acute respiratory viral infections: analysis and subgroup analysis from a Phase 4, randomised, placebo-controlled, double-blind study. *BMC Infect Dis.* 2016;16:648.
102. Estensoro I, Pérez-Cordón G, Sitjà-Bobadilla A, Piazzon MC. Bromodeoxyuridine DNA labelling reveals host and parasite proliferation in a fish-myxozoan model. *J Fish Dis.* 2018;41:651–62.
103. Piazzon MC, Estensoro I, Calduch-Giner JA, Del Pozo R, Picard-Sánchez A, Pérez-Sánchez J, Sitjà-Bobadilla A. Hints on T cell responses in a fish-parasite model: *Enteromyxum leei* induces differential expression of T cell signature molecules depending on the organ and the infection status. *Parasit Vectors.* 2018;11:443.
104. Haug K, Salek RM, Conesa P, Hastings J, de Matos P, Rijnbeek M, Mahendrakar T, Williams M, Neumann S, Rocca-Serra P, Maguire E, González-Beltrán A, Sansone SA, Griffin JL, Steinbeck C. MetaboLights—an open-access general-purpose repository for metabolomics studies and associated meta-data. *Nucl Acids Res.* 2013;41:D781–6.

Publisher's Note

Springer Nature remains neutral with regard to jurisdictional claims in published maps and institutional affiliations.

Ready to submit your research? Choose BMC and benefit from:

- fast, convenient online submission
- thorough peer review by experienced researchers in your field
- rapid publication on acceptance
- support for research data, including large and complex data types
- gold Open Access which fosters wider collaboration and increased citations
- maximum visibility for your research: over 100M website views per year

At BMC, research is always in progress.

Learn more biomedcentral.com/submissions

